ChemComm

RSC Publishing

COMMUNICATION

View Article Online
View Journal | View Issue

Cite this: *Chem. Commun.*, 2013, **49**, 5832

Received 17th April 2013,
Accepted 8th May 2013

DOI: 10.1039/c3cc42841a

www.rsc.org/chemcomm

A new route for the preparation of mesoporous carbon materials with high performance in lithium–sulphur battery cathodes†

Martin Oschatz,[a] Sören Thieme,[b] Lars Borchardt,[a] Martin R. Lohe,[a] Tim Biemelt,[a] Jan Brückner,[b] Holger Althues[b] and Stefan Kaskel*[ab]

A novel method for the preparation of highly mesoporous carbon materials (Kroll-Carbons; KCs) is described based on reactive carbochlorination etching of titania nanoparticles inside a dense carbon matrix leading to mesoporous carbons with precisely controllable porosity and high performance as cathode materials for lithium–sulphur (Li–S) batteries.

Porous carbon materials[1] play an essential role in air purification/gas separation processes,[2] catalysis,[3] gas storage,[4] and energy/environmental related applications.[5] While microporous carbons (pore diameter <2 nm) can be prepared in a wide range of pore sizes, uniformly structured mesoporous carbons (pore diameter from 2 to 50 nm) are not produced on a large scale because so far they are mostly used in niche applications such as the filtration of blood for the removal of inflammatory mediators[6] or in academic research. The pioneering work of Ryoo *et al.* established a new class of highly ordered mesoporous carbons using nanocasting of ordered mesoporous SiO_2 materials with carbon precursors and subsequent template removal by etching in hydrofluoric acid or sodium hydroxide solutions.[7] An advantageous soft templating approach for the direct synthesis of mesoporous carbons was developed by Zhao *et al.* by using the evaporation induced self-assembly (EISA) method.[8] In contrast to such complex templating approaches, physical or chemical activation processes do not allow precise control of mesopore sizes, and therefore an ultimate process for the generation of mesoporous carbons is still not available.

Especially in lithium–sulphur (Li–S) batteries,[9] mesoporous carbons are ideal conductive host structures for embedding the active material. Sulphur-based cathodes exhibit a broad operating temperature[10] as well as an intrinsic overcharge protection mechanism which greatly enhances the battery safety.[11] Carbon materials, prepared by classical templating approaches, have been investigated for that purpose. CMK-3 with uniform and ordered mesopores showed promising reversible capacities[12] and Liu and co-workers have optimized carbons with disordered mesopores for Li–S batteries.[13] Ordered mesoporous carbons synthesized by a soft templating approach cause improved cycle life and performance at a high rate of 1 C.[14] Mesoporous hollow carbon spheres[15] as well as spherical OMC nanoparticles with bimodal mesoporosity prepared from polymeric opal structures[16] were introduced as sulphur host for high rate Li–S batteries showing an excellent capacity.

In the following we present a new chemical method for the production of mesoporous carbon materials with very high internal pore volume of more than 3 $cm^3\ g^{-1}$, specific surface areas ranging close to 2000 $m^2\ g^{-1}$, and outstanding performance as cathodes in Li–S cells. They can be obtained by using high-temperature chlorination of titania in the presence of oxygen acceptors (also referred to as carbochlorination), which is the key step in the Kroll-process for the large-scale production of elemental titanium.[17] In the following, such mesoporous carbon materials are named Kroll-Carbons (KCs).

For the production of KCs, titanium dioxide nanoparticles (Degussa P25, measured SSA: 50 $m^2\ g^{-1}$) are mixed with sucrose as an inexpensive carbon precursor. The hydrocarbon undergoes an acid catalyzed polymerization, encapsulating the TiO_2 nanoparticles, and is subsequently thermally converted into a carbon network under inert conditions. The titanium dioxide template is removed by dosing chlorine gas into the TiO_2–carbon composite material according to the reaction $TiO_2 + 2\ Cl_2 + (2 + x)\ C \rightarrow TiCl_4 + 2\ CO + x\ C$, where the residual C represents the Kroll-Carbon (ESI,† Fig. S1). The useful by-product $TiCl_4$ can be removed at the end of the reactor by distillation. KCs are of high purity (more than 99.5 wt% of carbon) as shown by electron dispersive X-ray spectroscopy (EDX) measurements. Thermal analyses under air atmosphere indicate complete carbon combustion, and powder XRD measurements of the KCs only show the characteristic graphite (002) peak at moderate intensity, indicating the absence of impurities as well as a certain degree of graphitization in the pore walls of KCs (Fig. S2, ESI†). They differ from

[a] *Department of Inorganic Chemistry, Dresden University of Technology, Bergstrasse 66, D-01069 Dresden, Germany. E-mail: stefan.kaskel@chemie.tu-dresden.de; Fax: +49 351 46337287; Tel: +49 351 46333632*

[b] *Fraunhofer Institute for Material and Beam Technology, Winterbergstraße 28, D-01277 Dresden, Germany*

† Electronic supplementary information (ESI) available: Further material characterization; detailed electrochemical analysis and synthesis procedure of KCs. See DOI: 10.1039/c3cc42841a

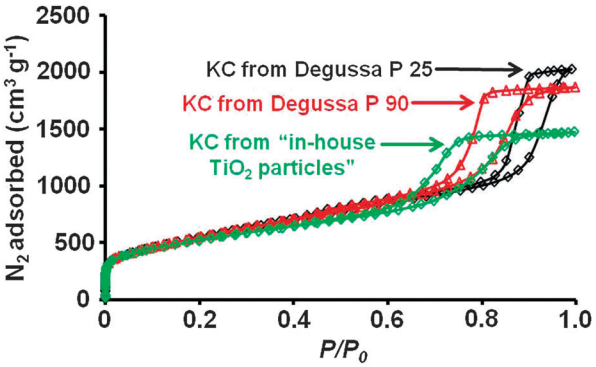

Fig. 1 Nitrogen physisorption isotherms (−196 °C) of KCs prepared from different TiO_2 templates.

carbide-derived carbons,[18] which are produced by high-temperature chlorine treatment of carbides, since TiC formation is not observed before chlorine treatment at 900 °C (Fig. S2, ESI†).

Obtained KCs show remarkably high specific BET surface areas of 1989 m^2 g^{-1} as shown by nitrogen physisorption measurements at −196 °C (Fig. 1, Table S1, and Fig. S3, ESI†). The resulting mesopores are uniform and highly accessible, resulting in a type IV isotherm with a distinctive H1 hysteresis loop. The over-all pore volume is as high as 3.1 cm^3 g^{-1} due to the high amount of large mesopores making this new material suitable for the infiltration of large amounts of sulphur. The pore size distribution (PSD) calculated by using a QSDFT kernel (Fig. S4, ESI†) shows a multimodal distribution of pore diameters with maxima at 1 nm, 4.2 nm, and 18 nm. While the large pores originate from the titanium dioxide template particles, the smaller mesopores arise from empty spaces between the TiO_2 nanoparticles due to incomplete filling of the template voids with precursor molecules during infiltration (Fig. S5, ESI†). Additionally, 0.3 cm^3 g^{-1} micropores (1 nm in diameter) are generated by the CO evolution in the Kroll reaction in analogy to physical activation procedures. The carbon matrix surrounding the template particles serves as an oxygen acceptor in the Kroll process and its gasification is responsible for the significantly higher specific surface areas when compared to other mesoporous carbons prepared using wet chemical removal of SiO_2 templates of similar size, which does not lead to the formation of micropores.[13]

Since the behavior and the performance of porous carbons in various applications strongly depends on the pore size, it is crucial for any synthetic route to allow control over the pore diameter as precisely as possible. In addition to Degussa P25, the KC synthesis was carried out with a series of template particles with higher specific surface areas corresponding to smaller particle size (Degussa P90, measured SSA: 100 m^2 g^{-1} and in-house made TiO_2 particles prepared by flame spray pyrolysis, measured SSA: 152 m^2 g^{-1}). The hysteresis loops in the nitrogen physisorption measurements shift towards lower relative pressures (Fig. 1) while the specific surface areas remain at the same level. The corresponding PSDs (Fig. S4, Table S1, ESI†) confirm the decreasing diameter of the large mesopores from 18 nm (Degussa P 25), to 11 nm (Degussa P 90), and 8.5 nm (in-house TiO_2 particles), showing the possibility to precisely control the mesopore sizes of KCs. The total pore volumes decrease due to the lower pore diameters while the micropore sizes and -volumes stay at the same level.

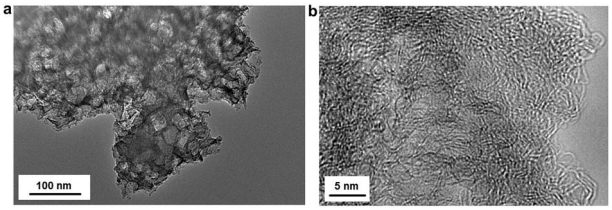

Fig. 2 TEM images of KCs prepared from Degussa P25 template particles.

SEM images of the KCs (Fig. S6, ESI†) show the presence of a distinctive arrangement of mesopores with block-shaped geometry and a foam-type structure which is responsible for the high internal pore volumes. The average sizes of the large mesopores in TEM images (Fig. 2a) is 15 to 25 nm and in good agreement with the nitrogen physisorption analysis. Moreover, the mesopore size is very close to the template dimensions (Fig. S7, ESI†) and the presence of some edges and corners of TiO_2 nanoparticles confirm the carbochlorination reaction as being highly conformal (Fig. S8, ESI†). TEM images at higher magnifications (Fig. 2b) show the carbon microstructure of the KCs as an arrangement of mostly disordered sp^2 carbon fringes.

Kroll-Carbons from Degussa P25 templates offer a very high mesopore volume. They were infiltrated with different amounts of sulphur by melt infiltration, and the resulting composite structures were characterized with regard to their applicability as Li–S cathodes. In the following, the cathodes are denoted as KC/S_53, KC/S_60, KC/S_64 and KC/S_72 according to their sulphur content in wt% (Table S2, ESI†). Their surface is smooth but reveals a wide-open and highly accessible inter-particular porosity throughout the active material layer (Fig. S9, ESI†). The KC/S weight ratios determined by TGA are in good accordance with the expected values since the melt infiltration strategy allows precise control over the KC/S composite composition (Fig. S9, ESI†). The powder XRD patterns of KC/S composite cathodes (Fig. S10, ESI†) show that sulphur is completely melt-infiltrated and well dispersed inside the KC framework, effectively suppressing the crystal growth of sulphur particles due to the high amount of mesopores.[12]

The cycling stabilities of KC/S composite cathodes with variable sulphur content were characterized by galvanostatic cycling (Fig. 3 and Fig. S11, ESI†) at a constant rate of 167 mA g^{-1} (C/10). Please note that all capacity values are given in terms of mA h g^{-1} per sulphur mass, if not mentioned separately. High initial discharge capacities of 1089 mA h g^{-1} (KC/S_53), 1115 mA h g^{-1} (KC/S_60), 1046 mA h g^{-1} (KC/S_64), and 1038 mA h g^{-1} (KC/S_72) were determined for all cathodes. After a capacity decay of maximal 18% within the first 10 discharge–charge cycles, the KC/S composites exhibit an excellent cycling stability with highly consistent capacities of 806 mA h g^{-1} (KC/S_53), 820 mA h g^{-1} (KC/S_60), 817 mA h g^{-1} (KC/S_64), and 736 mA h g^{-1} (KC/S_72) after 80 cycles. For all composites, more than 70% of the initial discharge capacity can be reversibly utilized even at a very high sulphur loading of 72 wt% and at a low rate of C/10, although this is a combination which is known to cause extensive active material loss by lithium polysulfide shuttling and rupturing of the electrically conductive carbon backbone.[19] The sulphur utilization is highly stable at approximately 50% and nearly independent of

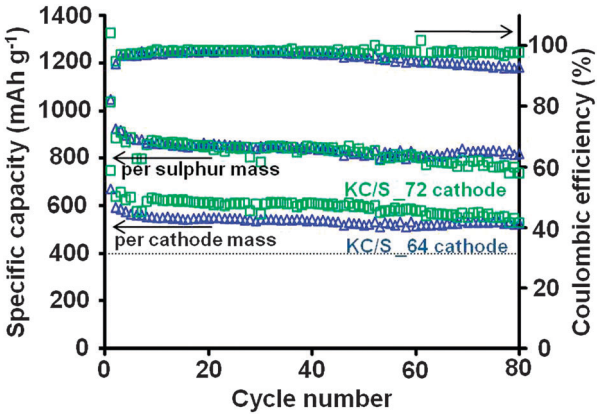

Fig. 3 Cycling stabilities and coulombic efficiencies of the KC/S_64 (triangles) and KC/S_72 (squares) cathodes.

the amount of sulphur stored in the composite, since the 1 nm micropores and small 4.2 nm mesopores within the hollow KC walls are highly favorable for adsorption and contacting of sulphur species due to the high specific surface area. On the other hand, the high pore volume provided by the large 18 nm mesopores guarantees effective storage of nanometer-sized sulphur particles and fast lithium ion diffusion. KC/S_72 is most suitable for the application in energy storage systems since the initial discharge capacity of 747 mA h g^{-1} per cathode mass (including binder and conducting agent) is much higher compared to cathodes with lower sulphur content, making it both the more practical and cheaper choice since less host material is needed. Only a slight decrease in the cell discharge voltage is observed when the cathode is loaded with extraordinary high amounts of sulphur (72 wt%). This indicates that sufficient amounts of Li^+ ions and electrons can diffuse to all reaction sites, facilitating the electrochemical conversion of sulphur at the large C/S interface area within Kroll-Carbon (Fig. S12, ESI†).

A comparison of the electrochemical behavior of KCs with the well known mesoporous material CMK-3 (Fig. S13, ESI†) clearly shows the high potential of the new class of mesoporous carbons in Li–S cathodes (Fig. S14, ESI†). The CMK-3/S_53 and CMK-3/S_60 reference electrodes show significantly lower capacitance as compared to the KC/S_72 cathode at even lower sulphur loadings. Especially when the capacity related to the mass of the whole cathode is considered, the performance of Kroll-Carbon-based electrodes significantly exceeds that of CMK-3. This can be explained by the significantly higher pore volume and specific surface area of the KC leading to a rather complete utilization of encapsulated sulphur due to the large C/S interface and sufficient hollow space for electrolyte penetration and volume expansion. It should be mentioned that the electrochemical results of the ordered mesoporous reference material are in good accordance with the results presented by Nazar *et al.* and that a higher sulphur loading within this material is not achievable due to its limited porosity.

The KC/S_72 cathode laminated onto carbon-coated expanded aluminum current collector (CC) with about 3.0 mg (ED/Al) cm^{-2} exhibits a high active material: a CC weight ratio of 3.3 : 1 leading to a very high capacity exceeding 450 mA h g^{-1} related to the cathode weight including the CC at C/10. Furthermore, very high current densities of 8.23 mA cm^{-2} (1 C) can be delivered when sacrificing a lot of the available capacity (feasible capacity: 110 to 160 mA h g^{-1} related to the electrode mass; Fig. S15, ESI†).

The Kroll-type reaction scheme using flame derived TiO_2 nanoparticles as templates results in carbons with high specific surface area and pore volumes up to 1980 $m^2 g^{-1}$ and 3.1 $cm^3 g^{-1}$, respectively. The synthesis process is highly versatile for tailoring the pore morphology and diameter in a wide range. The novel materials prepared from a commercially available template material (Degussa P 25) show outstanding performance as sulphur host material in high capacity cathodes for lithium–sulphur batteries. Extremely high sulphur contents up to 72 wt% cause initial discharge capacities up to 747 mA h g^{-1} and stable cycling with reversible capacities of more than 550 mA h g^{-1} (related to the mass of the cathode).

Even though various mesoporous carbon materials show excellent performance as cathode materials in Li–S cells, all of them are derived by classical templating approaches and are thus difficult to produce on a larger scale. In our view, the Kroll-process, and especially the carbochlorination, is a valuable new process for upscaling the synthesis of mesoporous carbons with well-defined pore size. Even though chlorination at high temperatures is a dangerous and toxic process, the low price of chlorine and the possibility of reusing the by-product $TiCl_4$ are highly attractive.

Financial support by the project ''Nanomaterials for future generation Lithium Sulphur batteries'' (''MaLiSu'') is gratefully acknowledged.

Notes and references

1 M.-M. Titirici and M. Antonietti, *Chem. Soc. Rev.*, 2010, **39**, 103; Y. Gogotsi, *Carbon Nanomaterials*, CRC Press LLC, Boca Raton, 2006.
2 F. Schueth, K. S. W. Sing and J. Weitkanp, *J. Handbook of Porous Solids*, Wiley-VCH Verlag GmbH & Co. KGaA, Weinheim, 2002, vol. 3.
3 F. Rodriguez-Reinoso, *Carbon*, 1998, **36**, 159.
4 L. Schlapbach and A. Zuettel, *Nature*, 2001, **414**, 353.
5 P. Simon and Y. Gogotsi, *Nat. Mater.*, 2008, **7**, 845.
6 G. Yushin, E. N. Hoffman, M. W. Barsoum, Y. Gogotsi, C. A. Howell, S. R. Sandeman, G. J. Phillips, A. W. Lloyd and S. V. Mikhalovsky, *Biomaterials*, 2006, **27**, 5755.
7 F. Kleitz, S. H. Choi and R. Ryoo, *Chem. Commun.*, 2003, 2136; M. Kruk, M. Jaroniec, T.-W. Kim and R. Ryoo, *Chem. Mater.*, 2003, **15**, 2815.
8 Y. Meng, D. Gu, F. Zhang, Y. Shi, H. Yang, Z. Li, C. Yu, B. Tu and D. Zhao, *Angew. Chem., Int. Ed.*, 2004, **44**, 7053.
9 L. F. Nazar and X. Li, *J. Mater. Chem.*, 2010, **20**, 9821.
10 Y. V. Mikhaylik and J. R. Akridge, *J. Electrochem. Soc.*, 2003, **150**, A306.
11 J. R. Akridge, Y. V. Mikhaylik and N. White, *Solid State Ionics*, 2004, **175**, 243.
12 X. Ji, K. Lee and L. F. Nazar, *Nat. Mater.*, 2009, **8**, 500.
13 X. Li, Y. Cao, W. Qi, L. V. Saraf, J. Xiao, Z. Nie, M. Jaroniec, J.-G. Zhang, B. Schwenzera and J. Liu, *J. Mater. Chem.*, 2011, **21**, 16603.
14 G. He, X. Ji and L. F. Nazar, *Energy Environ. Sci.*, 2011, **4**, 2878.
15 N. Jayaprakash, J. Shen, S. S. Moganty, A. Corona and L. A. Archer, *Angew. Chem., Int. Ed.*, 2011, **50**, 5904.
16 J. Schuster, G. He, B. Mandlmeier, T. Yim, K. T. Lee, T. Bein and L. F. Nazar, *Angew. Chem., Int. Ed.*, 2012, **51**, 3591.
17 W. Kroll, *Patent US*, 2205854, 1940.
18 V. Presser, M. Heon and Y. Gogtsi, *Adv. Funct. Mater.*, 2011, **21**, 810; M. Oschatz, L. Borchardt, M. Thommes, K. A. Cychosz, I. Senkovska, N. Klein, R. Frind, M. Leistner, V. Presser, Y. Gogotsi and S. Kaskel, *Angew. Chem., Int. Ed.*, 2012, **51**, 7577.
19 S.-R. Chen, Y.-P. Zhai, G.-L. Xu, Y.-X. Jiang, D.-Y. Zhao, J.-T. Li, L. Huang and S.-G. Sun, *Electrochim. Acta*, 2011, **56**, 9549; B. H. Jeon, J. H. Yeon, K. M. Kim and I. J. Chung, *J. Power Sources*, 2002, **109**, 89.

